Organic LETTERS

Letter

pubs.acs.org/OrgLett

Dipeptide Nanotubes Containing Unnatural Fluorine-Substituted $\beta^{2,3}$-Diarylamino Acid and L-Alanine as Candidates for Biomedical Applications

Andrea Bonetti,[†,⊥] Sara Pellegrino,[*,†,⊥] Priyadip Das,[‡] Sivan Yuran,[‡] Raffaella Bucci,[†] Nicola Ferri,[§,#] Fiorella Meneghetti,[†] Carlo Castellano,[∥] Meital Reches,[‡] and Maria Luisa Gelmi[†]

[†]Department of Pharmaceutical Sciences, [§]Department of Pharmacological and Biomolecular Sciences, and [∥]Department of Chemistry, University of Milan, Milano 20122, Italy

[‡]Institute of Chemistry, The Hebrew University of Jerusalem, Jerusalem 91904, Israel

[#]Multimedica IRCCS, Milano 20099, Italy

Supporting Information

ABSTRACT: The synthesis and the structural characterization of dipeptides composed of unnatural fluorine-substituted $\beta^{2,3}$-diarylamino acid and L-alanine are reported. Depending on the stereochemistry of the β amino acid, these dipeptides are able to self-assemble into proteolytic stable nanotubes. These architectures were able to enter the cell and locate in the cytoplasmic/perinuclear region and represent interesting candidates for biomedical applications.

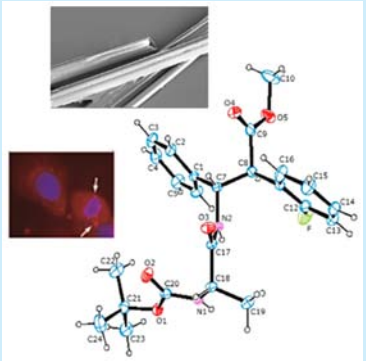

The construction of well-defined nanostructures from the self-assembly of small organic molecules has gained increasing attention in the past decade with the development of a broad range of applications, from catalysis to electrochemistry, biology, and nanotechnology.[1] In particular, peptide-based nanostructures are of valuable interest in biological systems,[2] e.g., as antimicrobials, as antiamyloidogenic agents, as transmembrane pore models, as ion-channel mimics, and as drug delivery vehicles. Nanotubes have been obtained by the self-assembly of different classes of peptides, including cyclic peptides, amyloid peptides, and surfactant-like peptides, as recently reviewed.[3] The diphenylalanine dipeptide (FF) has been widely exploited giving access to several ordered and almost intricate morphologies.[3,4] In aqueous solution it forms channel structures that are held together by a complex interplay of backbone−backbone hydrogen bonds and $\pi-\pi$ interactions between the aromatic rings of the side chains.[5] As a result, the obtained nanoscale tubes are characterized by hydrophobic external walls, while hydrophobic/hydrophilic groups remain exposed on the inner surface. These FF nanotubes have been proposed as potential drug delivery systems since they can self-assemble on a larger scale to form bundles comprising microscale tubular arrangements.[6] On the other hand, FF nanotubes show proteolytic degradation (70%, 24 h). Recently, it has been reported that the insertion of non-natural β-phenylalanine increases the resistance to protease degradation.[2b]

The aim of the present work has been the preparation of proteolytic stable nanotubes that could thus be exploitable in biomedical applications. Continuing our research on unnatural amino acids,[7] and on their use for the preparation of peptidomimetics,[8] we focused our attention on $\beta^{2,3}$-diarylamino acids, recently prepared in our group through a diasteroselective synthesis.[7a] In particular, we selected *syn* 3-amino-2-(2-fluorophenyl)-3-phenylpropanoic acid. This amino acid possesses all the features to be used for the preparation of self-assembled structures, i.e., the presence of aryl groups inducing $\pi-\pi$ interactions, the fluorine atom increasing lipophilicity, and due to its extended conformation,[9] the potential to favor β-sheet tapes.[2a] Furthermore, as a non-natural amino acid, resistance to proteolysis could be expected.[10]

Dipeptides **D1** and **D2**, containing L-Ala and the *S,S* or *R,R* stereoisomer of 3-amino-2-(2-fluorophenyl)-3-phenylpropanoic acid, respectively, were efficiently synthesized on a gram scale from racemic β-amino acid *syn*-**1** (see Scheme 1 and the Supporting Information for experimental details). Dipeptides **D1** and **D2** were fully characterized by NMR ($CDCl_3$, 500 MHz). As expected, the β-amino acid in both dipeptides is characterized by a *trans* conformation according to $^3J_{C\beta H-C\alpha H}$ values (10 Hz) that are typical of *syn* $\beta^{2,3}$-amino acids.[9] Only slight differences on the

Received: July 24, 2015
Published: September 3, 2015

DOI: 10.1021/acs.orglett.5b02132
Org. Lett. 2015, 17, 4468−4471

Scheme 1. Synthesis of D1 and D2

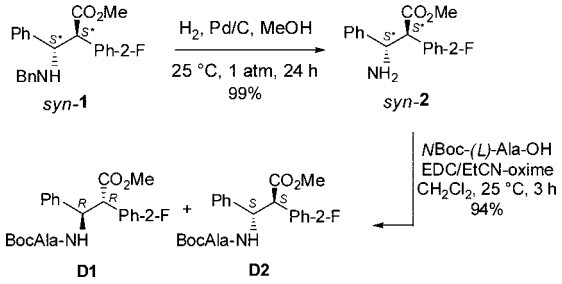

chemical shifts as well as on the NOEs were observed (Figure S1). A strong NOE effect between CH_{Ala1} and NH-2 was observed for both **D1** and **D2** dipeptides. The ^{1}H NMR experiments at variable temperatures and the DMSO-d_6 titrations excluded the presence of any intramolecular hydrogen bonds (see the Supporting Information: Figure S4B and discussion).

The CD signature of **D1** in H_2O/TFE (1:1) solution showed two positive bands at ∼197 and 215 nm. The **D2** spectrum presented the same Cotton effect but with opposite sign and slightly lesser intensity (Figure 1). Considering that in both

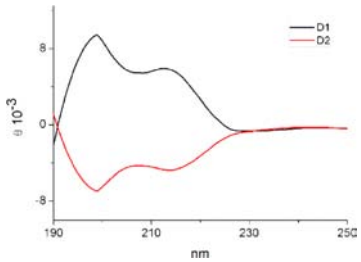

Figure 1. CD spectra of **D1** (black line) and **D2** (red line).

dipeptides alanine possesses the same L stereochemistry, this result indicates that the adopted conformation in solution is driven by the stereochemistry of the unnatural residue (*R,R* for **D1** and *S,S* for **D2**). CD analysis does not provide information on the conformation of the peptide because of the strong absorbance of the aromatic rings at 210 nm, as shown by UV analysis (see Figure S2, Supporting Information).

To gain further insight into the secondary structural information on the monomeric forms of **D1** and **D2**, we utilized Fourier transform infrared (FT-IR) analysis and deconvoluted each spectrum (Figure 2).

The FT-IR spectra of **D1** show two major peaks in the amide I region at 1688 and 1664 cm^{-1} indicating a β-turn conformation.

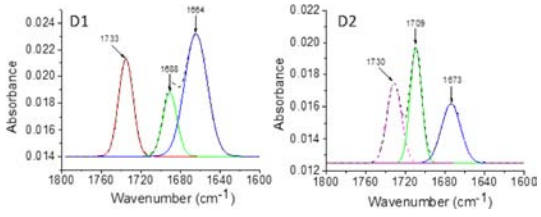

Figure 2. Deconvoluted FT-IR spectra of **D1** (left) and **D2** (right) in their monomeric form. The dashed line indicates the original FTIR spectra and the solid line represents the deconvoluted curves with a Gaussian function.

In the same region, the spectra of the **D2** peptide exhibited one peak at 1673 cm^{-1}, which corresponds to a β-turn.

Furthermore, the self-assembly behavior of **D1** or **D2** dipeptides in water was also investigated. To trigger the self-assembly, a stock solution of the dipeptides in HFP (100 mg/mL) was diluted with water to a final concentration of 2 mg/mL. These conditions were demonstrated before self-assembly of other aromatic peptides was allowed.[4c,d] Microscopic analysis showed that only **D2** can form ordered tubular structures (Figure 3). These structures (**NT-D2**) have a nanometric diameter and a high aspect ratio, therefore, they could be detected by optical microscopy (Figure 3D).

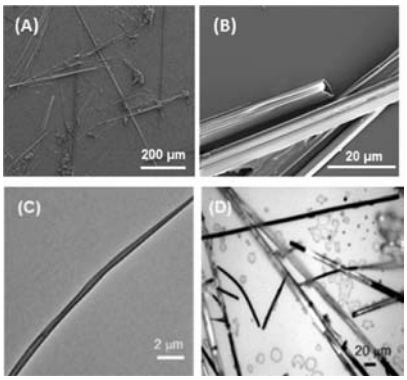

Figure 3. Microscopic analysis of the self-assembled tubular structure formed by the **D2** peptide: (A) HR-SEM micrograph of the tubes; (B) high magnification HR-SEM micrograph; (C) TEM micrograph of an individual tube; (D) optical microscopic images of the tubular assemblies.

The secondary structure of **NT-D2** was also analyzed by FT-IR (see Figure S2B, Supporting Information). In the amide I region (1600−1700 cm^{-1}), the FT-IR spectra of **NT-D2** showed one major peak at 1673 cm^{-1} indicating a β-turn conformation and one minor peak at 1618 cm^{-1} that may correspond to an extended hydrated structure.[11]

The fluorescence spectroscopy analysis evidenced that the emission spectrum of **NT-D2** shows a peak at 290 nm (λ_{ext}= 260 nm) with higher emission intensity compared to monomeric **D2** that could correspond to $\pi-\pi^*$ stacking interactions of phenyl units (see Figure S2A, Supporting Information). The latter interactions sometimes lead to an enhancement of fluorescence, as the close proximity of the aromatic ring with the π electron cloud leads to orbital overlap and produces a new or an enhanced emission.[12] The observed fluorescence enhancement of **NT-D2** suggests that $\pi-\pi^*$ interactions between the aryl groups could be one of the prominent reasons for the formation of self-assembled nanotubes. This hypothesis is supported by the same results obtained for other peptide-based nanotubes containing Phe residues.[13]

In order to fully investigate the structural characteristics of **D2** in the solid state, a single-crystal X-ray analysis has been undertaken. Suitable needle-shape crystals of **D2** were obtained from slow evaporation, at 25 °C, of a MeCN/H_2O (1:1) solution. The crystallographic analysis provided the establishment of the *S,S*-stereochemistry of the β-residue (Figure 4). In the crystal structure of **D2**, the backbone adopts a curled conformation, with the Boc protecting group bent with respect to the plane of the β-peptide link, as shown by the torsion angles N2−C17−C18−N1 of −33(1)° and C17−C18−N1−C20 of −69(1)°. The alanine side chain protrudes on the same side of the fluorine-substituted

DOI: 10.1021/acs.orglett.5b02132
Org. Lett. 2015, 17, 4468−4471

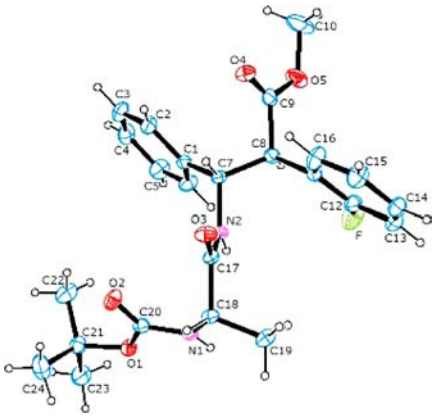

Figure 4. ORTEP[14] view of **D2** showing the arbitrary atom-labeling scheme. Displacements are at the 40% probability level.

ring, but it is oppositely oriented with respect to the C1−C6 phenyl moiety. The conformation of the molecule shows that the two aromatic rings are nearly parallel, forming a dihedral angle of 11(1)°. The two peptide links are in the *trans* configuration and show a slight deviation from planarity, as indicated by the torsion angles C7−N2−C17−C18 of 176(1)° and C18−N1−C20−O1 of 172(1)°. In the solid state, the strategic position of the fluorine contributed to enforcing the molecular packing through contact C5−H···F^{I} (^{I} at $-y + 2/3 + 1$, $x - y + 1/3$, $z + 1/3$), distance 3.003(3)Å, angle 153(1)°. The strongest hydrogen bond is intermolecular, between the peptide carbonyl group and the Boc-amide hydrogen of a neighbor molecule: N1−H···O3^{II} (^{II} at x,$+y$, $+z - 1$), 2.200(9) Å, angle 147(1)°, leading to chains along the c axis. These latter are connected by C6−H···O4^{II}, 2.394(9) Å, angle 173(1)°, and N2−H···O4^{II}, 2.742(9) Å, angle 149(1)° interactions.

In the crystal packing, weak contacts are also present between C13−H···O2^{III}, C14−H···O2^{III}, and C14−H···O3^{III} (^{III} at $-x + y + 1$, $-x + 2$, $+z$). This supramolecular organization generates a helix with three dipeptide molecules per turn, the screw axis of which is the crystallographic c axis (Figure 5). The formation of

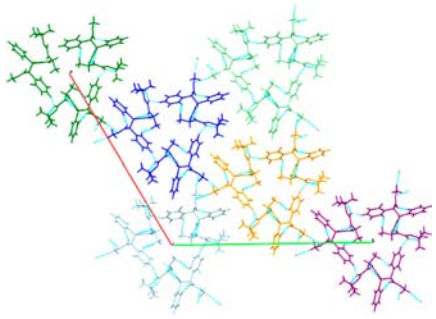

Figure 5. View down the c axis of the nanotubular organization in **D2** crystals (intermolecular interactions are marked as dashed lines).

the nanotubular architecture is mainly driven by the alignments of the carbonyl groups which permitted the self-assembly of the molecules in a straight line, with the N−H and C═O bonds aligned parallel to the tube length. These rods are held together by the Cπ−H···O, Cπ−H···F, and van der Waals interactions. The nanochannels have an average van der Waals diameter of about 4 Å, which is hydrophobic in nature, since they are internally decorated with the methylic side chains. Differently from what is observed in the fluorescence experiments, in the solid state there is no evidence supporting the presence of stacking interactions between the phenyl moieties, so the prevalent forces involved in the self-association in crystals are intermolecular hydrogen bonds that thus have the key role in the nanotube formation.

Considering the potential of the obtained nanotubes for biomedical applications, we investigated the stability of **NT-D2** to pronase from *Streptomyces griseus*, a highly nonspecific proteolytic enzyme.[15] Solutions of **NT-D2** (DMSO 20% v/v in PBS; pH = 5, 6, 7, 8; both in the presence or absence of pronase; incubation time of 48 h at 25 °C, see Figures S6 and S7, Supporting Information) were monitored by RP-HPLC.[16] No significant changes were observed, indicating that, owing to the presence of the unnatural amino acid, **NT-D2** nanotubes are stable to proteolytic degradation. The thermal stability of **NT-D2** in solution was tested by ^{1}H NMR experiments in DMSO-d_6 and in a wide range of temperatures (30−120 °C; Figure S8, Supporting Information). The sample was also maintained at 120 °C for 4 h. No significant structural changes were observed up to 120 °C, demonstrating also the thermal stability of the nanotubes in solution. In order to investigate whether **NT-D2** were efficiently incorporated into the cells, both flow cytometry and microscopy analyses were performed on dye-loaded derivatives. 5(6)-Carboxylfluorescein-**NT-D2** and rodhamine b (RhB)-**NT-D2** were thus obtained by incorporation these luminescent dyes during the self-assembly process of the **D2** peptide. In Figure 6, the fluorescence microscopic images of RhB-**NT-D2** are shown, indicating the loading of the RhB dye into the tubular structures.

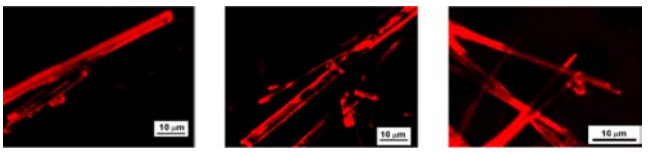

Figure 6. Fluorescence microscopic images of rodhamine labeled-**NT-D2** shows nanotubes with high aspect ratios, and the fluorescence suggests the presence of RhB across the tubular structures at the microscale.

For the flow cytometry determination, SMCs were incubated with 5(6)-carboxylfluorescein-**NT-D2** for 24 h and cell fluorescence determined after trypsinization of the cell monolayer. As shown in Figure 7A, cell fluorescence intensity, expressed as mean fluorescence index (MFI), increased in a concentration-dependent manner, from 1 to 100 μM, with no apparent saturation. The analysis with a fluorescent microscope

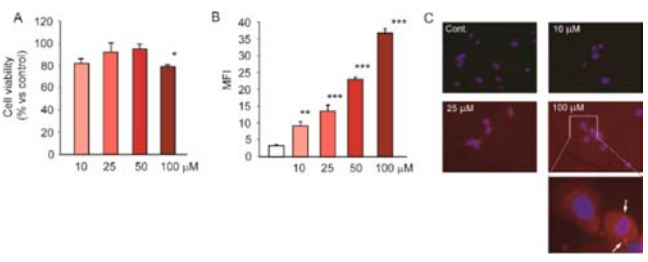

Figure 7. Cytotoxicity and cellular incorporation of **NT-D2**: (A) MTT assay performed after 48 h incubation with indicated concentrations of **NT-D2**; (B) flow cytometry analysis after incubation for 24 h with 5(6)-carboxylfluorescein-**NT-D2**; (C) fluorescent microscopy analysis after incubation for 24 h with rodhamine-**NT-D2**. *p < 0.05; **p < 0.01; ***p < 0.001 vs control, Student's t test.

DOI: 10.1021/acs.orglett.5b02132
Org. Lett. 2015, 17, 4468−4471

also revealed that at a concentration of 25−100 μM the rodhamine-**NT-D2** nanotubes were actively incorporated into the cells in the cytoplasmic/perinuclear region (Figure 7B). The lack of signal at the concentration of 10 μM was probably due to the less sensitive assay compared to the flowcytometric analysis.

The eventual cytotoxicity of the nanotubes was then investigated in cultured primary human smooth muscle cells (SMCs). This cell type was chosen because it is derived from human vessel, it represents the most abundant cell type directly exposed to a particular therapy once the circulating system is reached, and finally, it has high suitability and nonmalignant origin. The incubation for 48 h with **NT-D2** determined a statistically significant cytotoxic effect at 200 μM concentration with a reduction of cell viability of approximately 20% (Figure 7C, data not shown). No toxicity was detected at concentrations ranging from 1 to 100 μM.

In conclusion, in this work, we reported on the self-assembly of a dipeptide constituted by (*S,S*)-3-amino-2-(2-fluorophenyl)-3-phenylpropanoic acid and L-alanine. In the solid state, the nanotubular architecture is consolidated by intermolecular N−H···O hydrogen bonds, Cπ-H···O, Cπ-H···F, and van der Waals interactions. Finally, the presence of the unnatural β amino acid gives proteolytic and thermal stability to the obtained nanotubes. These assemblies are not cytotoxic at a concentration up to 50 μM and are incorporated into the cells. Taken together, these results indicate that that these supramolecular architectures could be exploitable for future biomedical applications.

■ ASSOCIATED CONTENT

Supporting Information

The Supporting Information is available free of charge on the ACS Publications website at DOI: 10.1021/acs.orglett.5b02132.

X-ray data for **D2** (CIF)

Experimental procedures and NMR characterization of **D1** and **D2** (PDF)

■ AUTHOR INFORMATION

Corresponding Author

*E-mail: sara.pellegrino@unimi.it.

Author Contributions

⊥A.B. and S.P. contributed equally.

Notes

The authors declare no competing financial interest.

■ ACKNOWLEDGMENTS

Funding for this work has been provided by MIUR (PRIN 2010-2011 - prot. 2010NRREPL), Università degli Studi di Milano (Piano Sviluppo), and by a Marie Curie Integration Grant. P.D. acknowledges the support of the Israel Council for Higher Education. S.Y. acknowledges the support of CAMBER. We thank Prof. G. Aldini and Mrs. C. Marinello (University of Milano, Department of Pharmaceutical Sciences, Milano, Italy) for recording of fluorescence spectra.

■ REFERENCES

(1) (a) Yao, W.; Yan, Y.; Xue, L.; Zhang, C.; Li, G.; Zheng, Q.; Zhao, Y. S.; Jiang, H.; Yao, J. *Angew. Chem.* **2013**, *125*, 8875−8879. (b) Torabi, S.-F.; Lu, Y. *Curr. Opin. Biotechnol.* **2014**, *28*, 88−95. (c) Zhang, L.; Qin, L.; Wang, X.; Cao, H.; Liu, M. *Adv. Mater.* **2014**, *26*, 6959−6964. (d) Xu, Y.; Zhang, B. *Chem. Soc. Rev.* **2014**, *43*, 2439−2450. (e) Garcia-Frutos, E. M. *J. Mater. Chem. C* **2013**, *1*, 3633−3645. (f) Yao, H.-B.; Gao, M.-R.; Yu, S.-H. *Nanoscale* **2010**, *2*, 323−334. (g) Huang, M.; Schilde, U.; Kumke, M.; Antonietti, M.; Colfen, H. *J. Am. Chem. Soc.* **2010**, *132*, 3700−3707.

(2) (a) Luo, J.; Abrahams, J. P. *Chem. - Eur. J.* **2014**, *20*, 2410−2419. (b) Panda, J. J.; Chauhan, V. S. *Polym. Chem.* **2014**, *5*, 4431−4436. (c) Parween, S.; Misra, A.; Ramakumar, S.; Chauhan, V. S. *J. Mater. Chem. B* **2014**, *2*, 3096−3106. (d) Montenegro, A.; Ghadiri, M. R.; Granja, J. R. *Acc. Chem. Res.* **2013**, *46*, 2955−2965. (e) Hourani, R.; Zhang, C.; van der Weegen, R.; Changyi, L. R.; Keten, S.; Helms, B. A.; Xud, T. *J. Am. Chem. Soc.* **2011**, *133*, 15296−15299. (f) Lalatsa, A.; Schätzlein, A. G.; Mazza, M.; Hang Le, T. B.; Uchegbue, I. F. *J. Controlled Release* **2012**, *161*, 523−536. (g) Ziserman, L.; Lee, H.-L.; Raghavan, S. R.; Mor, A.; Danino, D. *J. Am. Chem. Soc.* **2011**, *133*, 2511−2517. (h) Castelletto, V.; Hamley, I. V.; Perez, J.; Abezgauz, L.; Danino, D. *Chem. Commun.* **2010**, *46*, 9185−9187. (i) Gao, X.; Matsui, H. *Adv. Mater.* **2005**, *17*, 2037−2050. (l) Hamley, I. V.; Castelletto, V.; Moulton, C.; Myatt, D.; Siligardi, G.; Oliveira, C. L. P.; Pedersen, J. V.; Abutbul, I.; Danino, D. *Macromol. Biosci.* **2010**, *10*, 40−48. (m) Martin, C. R.; Kohli, P. *Nat. Rev. Drug Discovery* **2003**, *2*, 29−37. (n) Fernandez-Lopez, S.; Kim, H. S.; Choi, E. C.; Delgado, M.; Granja, J. R.; Khasanov, A.; Kraehenbuehl, K.; Long, G.; Weinberger, D. A.; Wilcoxen, K. M.; Ghadiri, M. R. *Nature* **2001**, *412*, 452−455.

(3) Hamley, I. W. *Angew. Chem., Int. Ed.* **2014**, *53*, 6866−6881.

(4) (a) Zou, Q.; Zhang, L.; Yan, X.; Wang, A.; Ma, G.; Li, J.; Mçhwald, H.; Mann, S. *Angew. Chem.* **2014**, *126*, 2398−2402. (b) Handelman, A.; Lavrov, S.; Kudryavtsev, A.; Khatchatouriants, A.; Rosenberg, Y.; Mishina, E.; Rosenman, G. *Adv. Opt. Mater.* **2013**, *1*, 875−884. (c) Yuran, S.; Razvag, Y.; Reches, M. *ACS Nano* **2012**, *6*, 9559−9566. (d) Reches, M.; Gazit, E. *Science* **2003**, *300*, 625−627.

(5) Guo, C.; Luo, Y.; Zhou, R.; Wei, G. *ACS Nano* **2012**, *6*, 3907−3918.

(6) Silva, R. F.; Araújo, D. R.; Silva, E. R.; Ando, R. A.; Alves, W. A. *Langmuir* **2013**, *29*, 10205−10212.

(7) (a) Bonetti, A.; Clerici, F.; Foschi, F.; Nava, D.; Pellegrino, S.; Penso, M.; Soave, R.; Gelmi, M. L. *Eur. J. Org. Chem.* **2014**, *2014*, 3203−3209. (b) Pellegrino, S.; Contini, A.; Gelmi, M. L.; Lo Presti, L.; Soave, R.; Erba, E. *J. Org. Chem.* **2014**, *79*, 3094−3102. (c) Penso, M.; Foschi, F.; Pellegrino, S.; Testa, A.; Gelmi, M. L. *J. Org. Chem.* **2012**, *77*, 3454−3461. (d) Gassa, F.; Contini, A.; Fontana, G.; Pellegrino, S.; Gelmi, M. L. *J. Org. Chem.* **2010**, *75*, 7099−7106.

(8) (a) Ruffoni, A.; Contini, A.; Soave, R.; Lo Presti, L.; Esposto, I.; Maffucci, I.; Nava, D.; Pellegrino, S.; Gelmi, M. L.; Clerici, F. *RSC Adv.* **2015**, *5*, 32643−32656. (b) Pellegrino, S.; Bonetti, A.; Clerici, F.; Contini, A.; Moretto, A.; Soave, R.; Gelmi, M. L. *J. Org. Chem.* **2015**, *80*, 5507−5516. (c) Pellegrino, S.; Contini, A.; Clerici, F.; Gori, A.; Nava, D.; Gelmi, M. L. *Chem. - Eur. J.* **2012**, *18*, 8705−8715. (d) Cabrele, C.; Clerici, F.; Gandolfi, R.; Gelmi, M. L.; Molinari, F.; Pellegrino, S. *Tetrahedron* **2006**, *62*, 3502−3508.

(9) Cheng, R. P.; Gellman, S. H.; DeGrado, W. F. *Chem. Rev.* **2001**, *101*, 3219−3232.

(10) Vlieghe, P.; Lisowski, V.; Martinez, J.; Khrestchatisky, M. *Drug Discovery Today* **2010**, *15*, 40.

(11) Litvinov, R. I.; Faizullin, D. Z.; Zuev, Y. F.; Weisel, J. W. *Biophys. J.* **2012**, *103*, 1020−1027.

(12) Xu, Z.; Jiten Singh, N.; Lim, J.; Pan, J.; Ha Na Kim, H. N.; Park, S.; Kim, K. S.; Yoon, J. *J. Am. Chem. Soc.* **2009**, *131*, 15528−15533.

(13) (a) Krysmann, M. J.; Castelletto, V.; McKendrick, J. E.; Clifton, L. A.; Hamley, I. W. *Langmuir* **2008**, *24*, 8158−8162. (b) Acuna, G. P.; Möller, F. M.; Holzmeister, P.; Beater, S.; Lalkens, B.; Tinnefeld, P. *Science* **2012**, *338*, 506−510.

(14) Farrugia, L. J. *ORTEP-3 for Windows*; University of Glasgow: Glasgow, 1997.

(15) Frackenpohl, F.; Arvidsson, P. I.; Schreiber, J. V.; Seebach, D. *ChemBioChem* **2001**, *2*, 445−455.

(16) Control experiments on *N*-acetyl-L-tyrosine ethyl ester showed that the enzyme maintains its activity under the described conditions.

DOI: 10.1021/acs.orglett.5b02132
Org. Lett. 2015, 17, 4468−4471